Assembly of Arbitrary Designer Heterostructures with Atomically Clean Interfaces

Keda Jin, Tobias Wichmann, Sabine Wenzel, Tomas Samuely, Oleksander Onufriienko, Pavol Szabó, Kenji Watanabe, Takashi Taniguchi, Jiaqiang Yan, F. Stefan Tautz, Felix Lüpke, Markus Ternes, and Jose Martinez-Castro*

Van der Waals heterostructures are an excellent platform for studying intriguing interface phenomena, such as moiré and proximity effects. Many of these phenomena occurring in such heterostructures' interfaces and surfaces have so far been hampered because of their high sensitivity to disorder and interface contamination. Here, it reports a dry polymer-based assembly technique to fabricate arbitrary designer van der Waals heterostructures with atomically clean surfaces. The key features of the suspended dry pick-up and flip-over assembly technique are: 1) the heterostructure surface never comes into contact with polymers, 2) the assemble is entirely solvent-free, 3) it is entirely performed in a glovebox, and 4) it only requires temperatures below 130 °C. By performing ambient atomic force microscopy and atomically-resolved scanning tunneling microscopy on example heterostructures, it demonstrates the fabrication of air-sensitive heterostructures with ultra-clean interfaces and surfaces. It envisions that, due to the avoidance of polymer melting, this technique is potentially compatible with heterostructure assembly under ultra-high vacuum conditions, which promises ultimate heterostructure quality.

1. Introduction

The mechanical assembly of van der Waals (vdW) heterostructures[1] is a key technology for studying the emerging phenomena occurring at interfaces between 2D materials.[2,3] The popularity of this method is based on the ease and speed with which heterostructures can be built in a virtually infinite number of possible combinations. The constant demand for cleaner and better devices has driven the successive refinement of the assembly techniques, with the aim to meet the criteria of reliability, cleanliness, and interface quality to an ever greater extent, despite the simultaneous increase in the complexity of the structures. Currently, the dry pick-up assembly of 2D materials[4] and related techniques[5–8] are the most widely used ones in this regard as they offer great versatility and yield high-quality

K. Jin, T. Wichmann, S. Wenzel, F. S. Tautz, F. Lüpke, M. Ternes,
J. Martinez-Castro
Peter Grünberg Institut (PGI-3)
Forschungszentrum Jülich
52425 Jülich, Germany
E-mail: j.martinez@fz-juelich.de
K. Jin, T. Wichmann, S. Wenzel, F. S. Tautz, F. Lüpke, M. Ternes, J. Martinez-Castro
Jülich Aachen Research Alliance
Fundamentals of Future Information Technology
52425 Jülich, Germany
K. Jin, M. Ternes, J. Martinez-Castro
Institute for Experimental Physics II B
RWTH Aachen
52074 Aachen, Germany

T. Wichmann, F. S. Tautz
Institute for Experimental Physics IV A
RWTH Aachen
52074 Aachen, Germany
T. Samuely, O. Onufriienko, P. Szabó
Centre of Low Temperature Physics, Faculty of Science
Pavol Jozef Šafárik University & Institute of Experimental Physics, Slovak Academy of Sciences
04001 Košice, Slovakia
K. Watanabe
Research Center for Electronic and Optical Materials
National Institute for Materials Science 1-1 Namiki
Tsukuba 305-0044, Japan
T. Taniguchi
Research Center for Materials Nanoarchitectonics
National Institute for Materials Science
1-1 Namiki, Tsukuba 305-0044, Japan
J. Yan
Materials Science and Technology Division
Oak Ridge National Laboratory
Oak Ridge TN 37831, USA

**ADVANCED
SCIENCE NEWS**

www.advancedsciencenews.com

**ADVANCED
MATERIALS
INTERFACES**

www.advmatinterfaces.de

heterostructures. The method of dry pick-up assembly proceeds as follows: A polydimethylsiloxane (PDMS) polymer stamp covered with a sticky polymer film is used to pick up 2D crystals exfoliated from bulk material onto a substrate, typically Si/SiO$_2$. While the polymer film has a strong adhesion over a certain temperature range, the PDMS is soft, allowing a controlled contact to the flakes and protecting them from damage. The heterostructure is then assembled from the top to the bottom, starting with the material that will eventually form the topmost layer. In the last step, the heterostructure is released by contacting the target substrate and melting the polymer. Alternatively, a polymer whose thermoplastic properties allows a melt-free release can be employed.[7] Crucially, standard dry pick-up assembly techniques require fully contacting the heterostructure surface with the polymer, which inevitably leaves polymer residues on the surface and interface (due to the in-diffusion of molten polymer) of the final heterostructure.[9] In particular, if the heterostructure surface is formed by a reactive material, the contact with the polymer will degrade its surface.

A strategy to circumvent this problem is the use of a protective layer, i. e., an inert material that is placed as the topmost layer of the heterostructure to protect (encapsulate) the layers underneath from degradation.[6,10–12] In this case, the polymer residues can be removed from the protective layer with a combination of solvents such as chloroform, acetone or isopropanol, and the trapped bubbles in the interface can be removed with AFM-based mechanical cleaning methods.[13,14] The combination of inert encapsulation layers with such cleaning methods has been demonstrated to allow contamination-sensitive surface science techniques to be applied successfully.[15,16] Nevertheless, protective layers can pose a limit to the accessibility of the underlying material due to their finite thickness and electronic properties that can mask those of the underlying materials.

An alternative to avoid polymers to come into contact with the heterostructure surface is to assemble it in reverse order and to flip it over after the assembly process.[17–19] Using such techniques, the vdW heterostructure is typically released by melting the polymer layer (polypropylene carbonate, PPC) that is used during assembly, leaving a thick PPC layer underneath the finished heterostructure. The PPC is then removed by annealing at 250 °C in vacuum. Unfortunately, while the dry-transfer flip technique is a huge step forward, it also has its limitations: 1) The assembled heterostructure must be annealed in high vacuum for several hours to properly remove the residual PPC layer from underneath the heterostructure. Such extended annealing can cause atomic defects on the heterostructure surface.[18] 2) The required annealing temperature of 250 °C is incompatible with many 2D materials which degrade at this temperature.[20] 3) The large amount of PPC that must be evaporated makes it incompatible with ultra-high vacuum (UHV) environments, which are sensitive to organic contaminants.

Here, we present a novel technique for the mechanical assembly of ultra-clean vdW heterostructures that overcomes the drawbacks of existing assembly methods. Our suspended dry pick-up and flip-over assembly technique does not require the use of a protective encapsulation layer, nor does it require additional cleaning by solvents or AFM. Using ambient AFM and low-temperature STM, we demonstrate that atomically clean surfaces and interfaces are achievable for a variety of heterostructures.
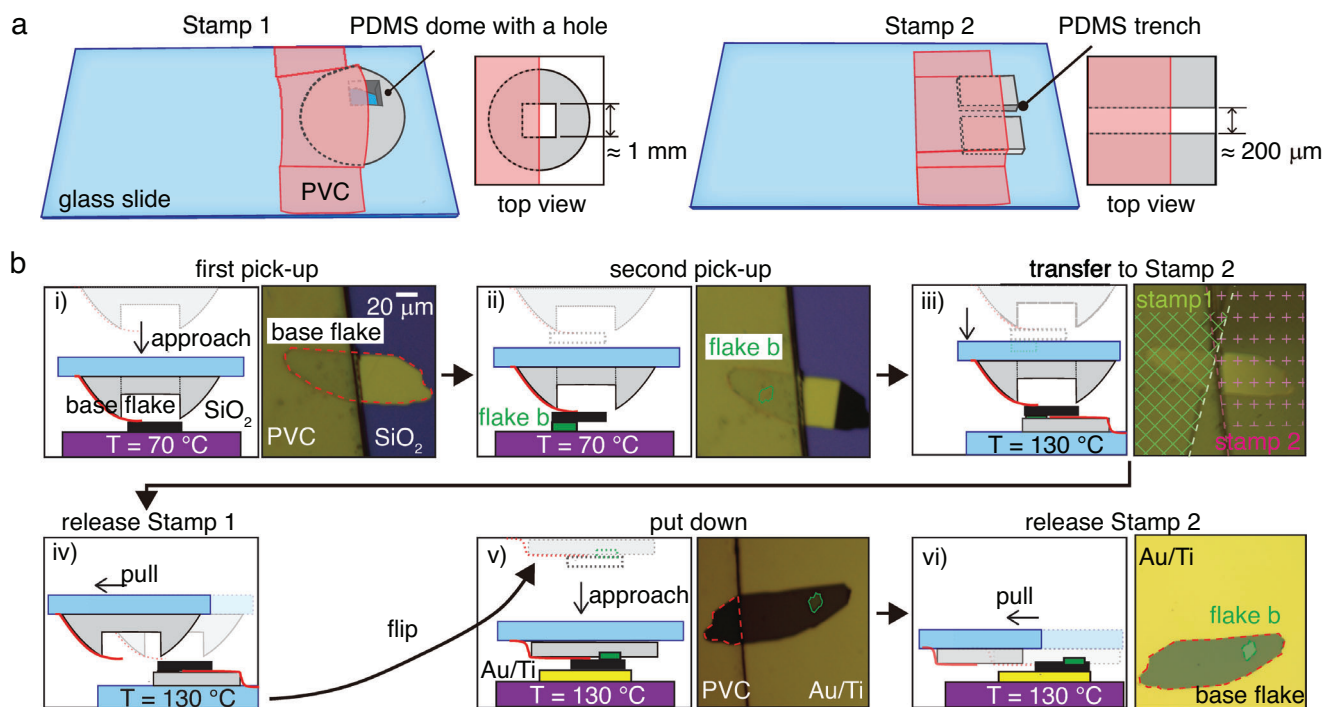
2. Results and Discussion

2.1. Description of the Suspended Dry Pick-Up and Flip-Over Assembly Technique

We start by preparing two PDMS stamps. The first one (stamp 1) is used to assemble the vdW heterostructure, while the second one (stamp 2) is used to flip and controllably place the vdW heterostructure onto the target substrate. Stamp 1 uses a dome-shaped PDMS, with an approximately 1×1 mm^2 square depression cut into its center, and is supported on a microscope glass slide (left panel of **Figure 1**a). Stamp 2 consists of a flat, 5 mm thick PDMS block that has been cut into two pieces with a scalpel, resulting in a trench of approximately 200 µm width (Figure 1a right panel) that exposes the supporting glass slide. For more details on the transfer slide preparation, see Figure S1 (Supporting Information).

Next, we prepare the polymer films that will be used for pick-up, flip-over, and release of the vdW heterostructure. To this end, a commercial poly(vinyl chloride) (PVC) film (RIKEN WRAP, Riken Fabro Corp)[7] is first annealed to 130 °C for one minute on a hot plate. This step is crucial because it prevents any uncontrolled thermal shrinkage of the PVC when mounted on the stamps and heated during subsequent steps (Figure S2, Supporting Information). After annealing, we transfer the PVC film onto a 1×1 cm^2 square of standard double-sided scotch tape, taking care not to wrinkle the film. The double-sided tape provides support and stability when manipulating the PVC film. Subsequently, we cut the PVC film into two pieces and place one of them on PDMS stamp 1, the other on PDMS stamp 2 (see Figure S3, Supporting Information), covering half of the square depression and half of the trench as shown in Figure 1a. Note that, both, the detailed shape of the PDMS stamps as well as the total contact area of the PVC films with the PDMS determine the stiffness of the suspended PVC films. In detail, we have observed that stiffer films show stronger adhesion with 2D materials. Thus, by placing the PVC on the two stamps such that the suspended area on stamp 1 is larger than on stamp 2, we promote stronger adhesion between polymer and heterostructure on stamp 2 compared to stamp 1. This crucial feature enables us to transfer the assembled vdW heterostructure from stamp 1 to stamp 2 later in the process, despite them being chemically identical PVC films.

Employing the two stamps, we assemble the vdW heterostructure in reverse order using a standard assembly stage (HQ graphene) as described in Figure 1b. We note that the first flake to be picked up, the base flake, should be thicker than ≈ 40 nm to provide the necessary stiffness and mechanical support for the subsequently following layers of the heterostructure. We contact the base flake with stamp 1 at 70 °C by touching roughly half of the flake with the PVC film (red) and then carefully pulling the stamp up vertically (panel (i) in Figure 1b; Video S1, Supporting Information). Subsequently, we pick up subsequent flakes by vdW interaction[5] at 70 °C to assemble the desired heterostructure. For each additional pick-up step, we make sure that the flake does not extend over the edge of the base flake (panel (ii) in Figure 1b; Video S2, Supporting Information).

Once the assembly of the vdW heterostructure on stamp 1 is completed, we flip the heterostructure using stamp 2. To do this,

**ADVANCED
SCIENCE NEWS**

www.advancedsciencenews.com

**ADVANCED
MATERIALS
INTERFACES**

www.advmatinterfaces.de

Figure 1. Schematic representation of the suspended dry pick-up and flip-over assembly of a WSe_2/Graphite heterostructure. a) 3D representations (top view) of stamps 1 and 2, showing in detail how the two PVC films (red) are suspended with the aid of the carved PDMS structures (grey). b) Flow diagram of the heterostructure assembly. i) Stamp 1 is brought into contact with the base flake (here graphite) at 70 °C by touching the left half of the base flake (black) with the PVC film (red). The base flake is then picked up by carefully retracting stamp 1 vertically. ii) The van der Waals heterostructure is assembled by contacting the exfoliated flake b (green, WSe_2), initially located on the SiO_2 substrate (purple), with the part of the base flake that is located directly underneath the PVC film. iii) The base flake on stamp 1 is brought into contact with stamp 2 at 130 °C, making sure that each stamp touches roughly half of the base flake (white and red dashed lines). iv) The van der Waals heterostructure is transferred by sliding stamp 1 sideways until the base flake is only in contact with stamp 2. v) After flipping the heterostructure upside down, stamp 2 with the heterostructure is mounted in the micro-manipulator stage. Subsequently, stamp 2 is brought into contact with the target substrate Au/Ti (yellow) on SiO_2 (purple) at 130 °C. vi) The heterostructure is finally released from stamp 2 by sliding the latter sideways and retracting it vertically.
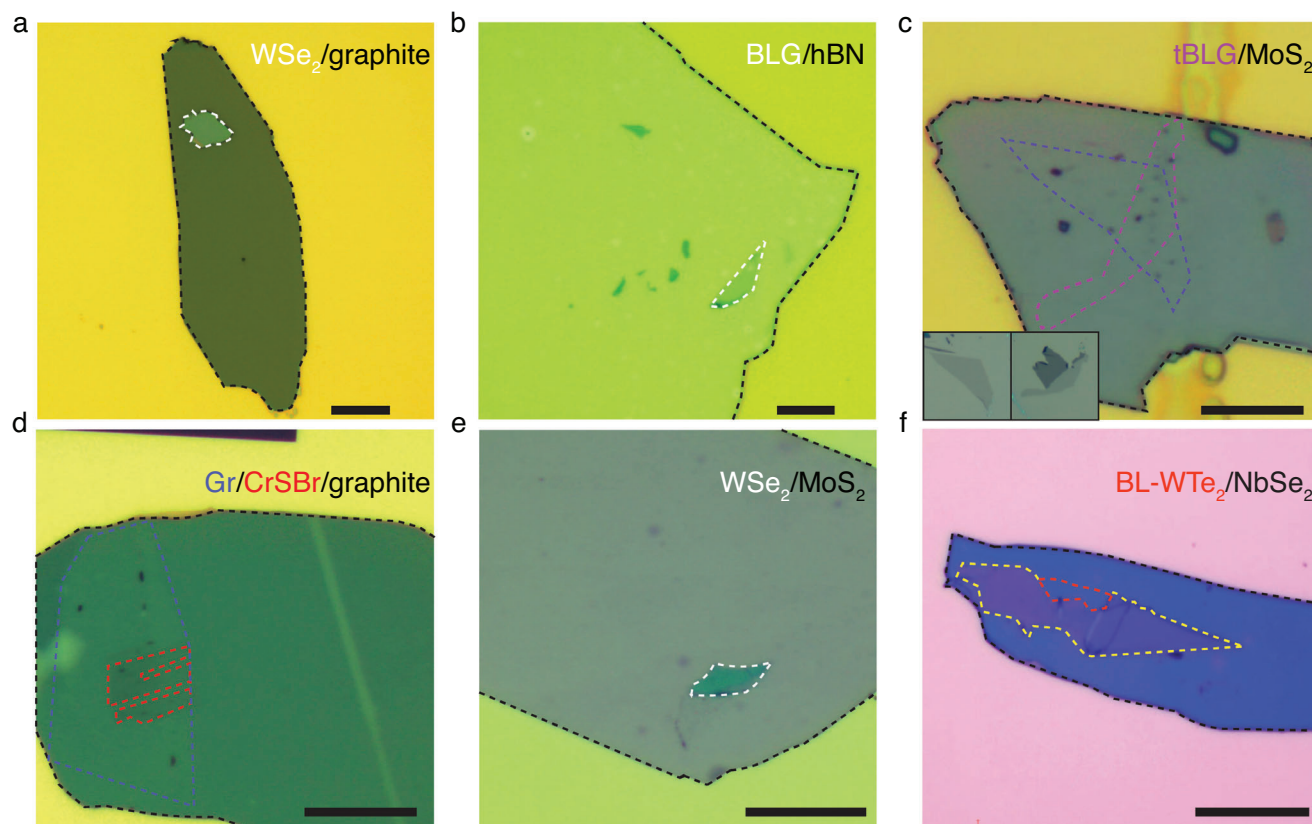
we place stamp 2 on the transfer stage and raise the temperature to 130 °C. We then carefully bring stamp 1 into contact with stamp 2, making sure that the PVC films on the two stamps only touch the base flake on opposite sides and not each other (panel (iii) in Figure 1b). Stamp 1 is then released by gently pressing and sliding it laterally (panel (iv) in Figure 1b; Video S3, Supporting Information). Next, stamp 2 is flipped over by mounting it into the micro-manipulator. The heterostructure is then brought into contact with the target substrate at 130 °C (panel (v) in Figure 1b). Finally, we release the vdW heterostructure by slowly moving stamp 2 laterally (panel (vi) in Figure 1b; Video S4, Supporting Information).

2.2. Arbitrary Designer Heterostructures

By assembling example heterostructures composed of a wide variety of different vdW materials, we demonstrate the broad applicability of our suspended dry pick-up and flip-over assembly technique. The used base flakes of the heterostructures include common materials typically used for optical, transport, and surface characterization experiments, such as hexagonal boron nitride (hBN), graphite, or MoS_2.[21–23] In addition, we demon-

strate that air-sensitive (reactive) materials, such as $NbSe_2$, can also be used as base flakes, although only the base flake surface area, which did not come into contact with the PVC film is atomically clean. **Figure 2** shows a summary of six example heterostructures: a) WSe_2 on graphite, the former being a transition metal dichalcogenide known to induce strong spin-orbit coupling into graphene[24]; b) bilayer graphene on hBN, the latter being an insulator, which is typically used for gating purposes[25]; c) twisted-bilayer graphene on MoS_2, assembled from two separate graphene monolayers that have been sequentially picked up with a controlled twist angle between them, allowing the simultaneous study of the strongly correlated physics of twisted-bilayer graphene and the proximity-induced strong spin-orbit coupling by the transition metal dichalcogenide[26]; d) graphene on CrSBr, the latter being a 2D antiferromagnetic semiconductor whose electronic interlayer coupling can be magnetically controlled[27]; e) WSe_2 on MoS_2, a semiconductor heterostructure that has been intensively studied for its optoelectronic properties[28]; f) WTe_2 on $NbSe_2$, a heterostructure that realizes 1D topological superconductivity.[18,29]

From the successful assembly of the heterostructures demonstrated here, we conclude that the suspended dry pick-up and flip-over assembly technique can be applied to a wide range of

2300658 (3 of 7)

ADVANCED
SCIENCE NEWS

www.advancedsciencenews.com

ADVANCED
MATERIALS
INTERFACES

Open Access

www.advmatinterfaces.de

Figure 2. Exemplary vdW heterostructures. All panels show optical microscopy images of various assembled heterostructures on Au covered SiO$_2$ substrates. The flake outlines are indicated as color-coded dashed lines. a) WSe$_2$ on graphite. b) Bilayer graphene (BLG) on hexagonal boron nitride (hBN). c) Twisted-bilayer graphene (tBLG) on MoS$_2$. Inset: optical images of the exfoliated graphene flakes prior to the assembly. d) Graphene (Gr) on CrSBr on graphite. e) WSe$_2$ on MoS$_2$. f) Multilayer WTe$_2$ on NbSe$_2$ where the bulk and bilayer (BL) areas are marked with yellow and red dashed lines, respectively. The scale bars are 20 µm in all panels.

materials including most of the common materials used for optics, electronic transport, and surface science studies. We note that, if there are any additional principal limitations at all, they will most likely be found in the vdW heterostructure assembly process itself: A too strong interaction between the exfoliated flakes and the SiO$_2$ substrate might prevent the pick-up by the base flake or previously picked-up layers on top of the base flake.

2.3. Surface and Interface Quality

To assess the quality of our assembled vdW heterostructures, we characterize the resulting surface and internal interface quality. To this end, we inspect the assembled vdW heterostructures with ambient condition contact-mode AFM (c-AFM), focusing here on those with top layers of either monolayer graphene (**Figure 3**a,b) or twisted bilayer graphene (Figure 3c,d), because compared to the thicker 2D materials, graphene is more prone to wrinkle and fold. Less-than-optimal transfer methods tend to produce more trapped blisters and wrinkles in the graphene, allowing a direct comparison between different mechanical assembly methods. We assess three different criteria: 1) The number and area of trapped blisters at the interface, 2) possible damage of the top-

most layer, such as ruptures, 3) the amount of residue left on the surface. In comparison to standard dry-transfer techniques, we find that a reverse assembly of vdW heterostructures generally results in a lower number of trapped blisters and protects the topmost surface from rupturing in agreement with earlier reports.[30] Furthermore, the overall higher stiffness of the heterostructure provided by the base flake contributes to better interfaces, because it avoids inhomogeneities and stress arising from flexing of the polymer film. Lastly, we do not observe any traces of residue or damage on the topmost graphene layer whatsoever. In fact, the only visible residues are located in the contact front between the PVC and the base flake (see Figure S4, Supporting Information).

To further compare the surface quality achieved with our suspended dry pick-up and flip-over assembly technique to standard dry-transfer methods, we assembled a heterostructure following Ref. [7], where the heterostructure surface comes in full contact with the PVC polymer, i.e., without flip. The surface of the resulting Gr/NbSe$_2$/graphite heterostructure (Figure S5, Supporting Information) exhibits substantial polymer residue as well as damaged regions where the graphene is partially ruptured. Additionally, the graphene/NbSe$_2$ interface shows a multitude of blisters, a signature of trapped polymer residues at the interface.[9]
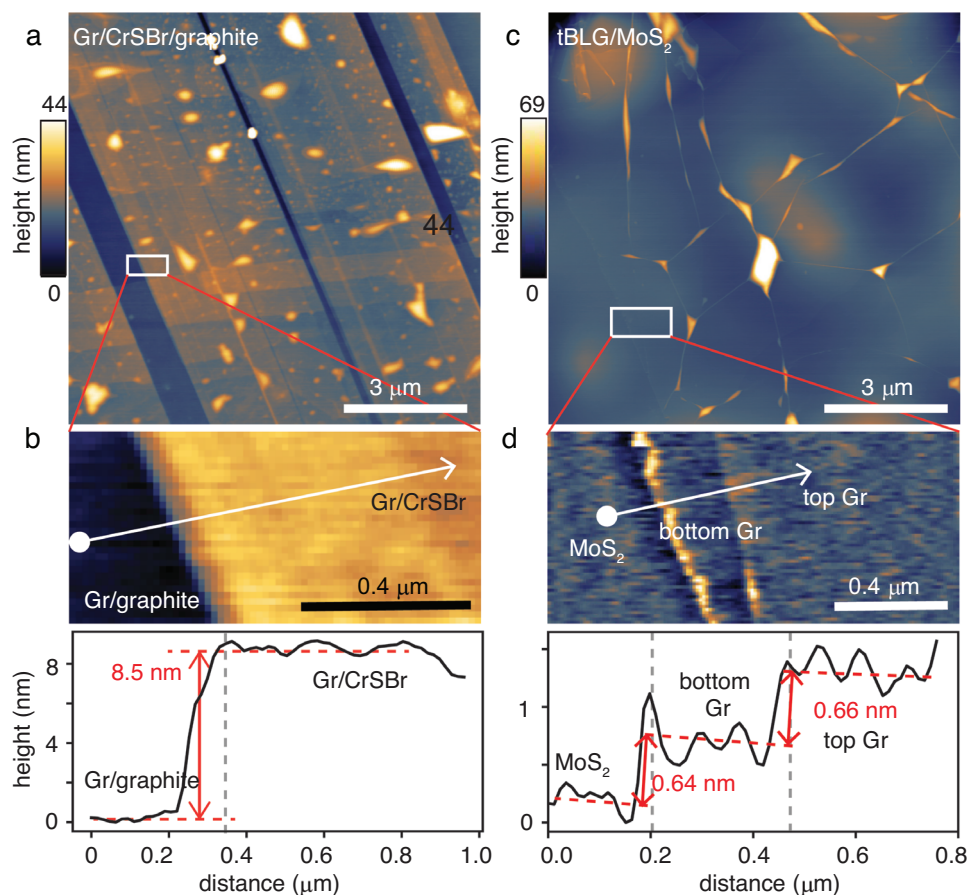
Figure 3. Atomic force microscopy on assembled vdW heterostructures. a) AFM topography of graphene on CrSBr on graphite. b) Zoom into the region highlighted by the white rectangle in panel a and topography cross-section along the white arrow. The thicknesses of the CrSBr steps are indicated. c) AFM topography of twisted-bilayer graphene on MoS_2. d) Zoom into the region highlighted by the white rectangle in panel (c), showing MoS_2 and the two graphene layers and topography cross-section along the white arrow. The thicknesses of the steps correspond to that of the graphene layers.

In contrast, the vdW heterostructures assembled with our suspended assembly technique do not show damage or surface contamination. Moreover, these heterostructures exhibit a reduced number of blisters, which also have a smaller radius. A detailed analysis of the AFM topographies in Figure 3b,d shows that their roughness is smaller than the noise of the c-AFM (RMS = 0.74 nm), demonstrating the flatness of the vdW heterostructures' interfaces assembled with this method.

2.4. Scanning Tunneling Microscopy

Finally, we analyze the surface quality and thus the compatibility of our suspended dry pick-up and flip-over assembly technique with contamination-sensitive surface science techniques like STM. For this, we inspect the $WTe_2/NbSe_2$ vdW heterostructure shown in Figure 2f. Since both $NbSe_2$ and WTe_2 are air-sensitive, the heterostructure was assembled in an argon-filled glovebox and transferred from there to the UHV chamber hosting the STM in a vacuum suitcase. For a detailed atomic-level evaluation of the surface cleanliness, measurements at three distinct sites were conducted: bulk $NbSe_2$, bulk WTe_2 and bilayer WTe_2. **Figure 4**a shows an atomically resolved image of $NbSe_2$—
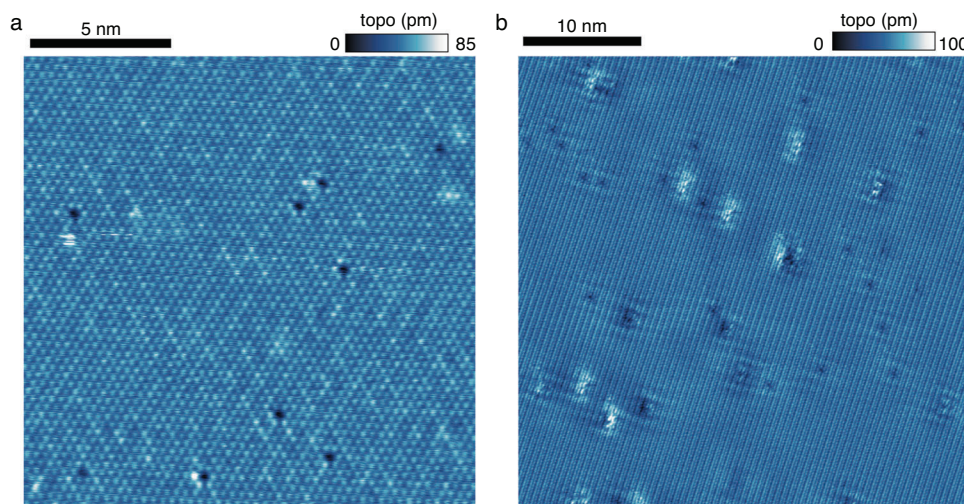
without any surface contaminants—and its 3×3 charge density wave, which emerges below $T_{CDW} = 32$ K and is known to be very sensitive to external perturbations.[31] In the same way, we were able to obtain atomically resolved images of the bilayer WTe_2 situated on the $NbSe_2$, again showing only single atomic defects (Figure 4b) and in different areas of the bilayer as well as on top of trapped blisters WTe_2 (Figure S6, Supporting Information).

We also analyzed the amount of polymer residue on the surface and the edge of bulk WTe_2 on $NbSe_2$. For this purpose, we measured a 2×2 µm^2 STM image topography corresponding to the maximum scanning range at 4 K (Figure S7a, Supporting Information), which points to the absence of polymer residue at the micrometer scale.

As a reference, we use PDMS to dry-transfer a bulk WTe_2 flake and examine its surface with STM. Figure S8 (Supporting Information) reveals a substantial PDMS residue on its surface, serving as a counter-example that shows the limitations of transfer techniques requiring full polymer contact.

3. Conclusion

The suspended dry pick-up and flip-over assembly technique allows the mechanical assembly of arbitrary designer vdW

ADVANCED
SCIENCE NEWS

www.advancedsciencenews.com

ADVANCED MATERIALS INTERFACES
Open Access

www.advmatinterfaces.de

Figure 4. Scanning tunneling microscopy on a BL WTe$_2$/NbSe$_2$ heterostructure. a) Atomic resolution STM topography on bulk NbSe$_2$ showing its 3 × 3 charge density wave (sample bias V_{bias} = 90 mV and tunneling current I_{set} = 100 pA). b) Atomic resolution STM topography on bilayer WTe$_2$ on bulk NbSe$_2$ (V_{bias} = 100 mV, I_{set} = 100 pA). Only a few single-atomic defects are observed on both surfaces, their abundance is close to the material's bulk defect concentration.

heterostructures with ultra-clean surfaces and interfaces. Notably, the method is suitable for heterostructure assembly in a glovebox and thus can be used for air-sensitive materials. The high quality of the resulting vdW heterostructures enables detailed surface studies, such as STM with atomic resolution even on air-sensitive materials, without requiring a protective layer. The reported assembly technique can be readily applied to the broad variety of available vdW materials and therefore can be applied in various research areas such as optics, electronic transport, and surface science. Because it does not require polymer melting nor chemical solvents, it also constitutes a potential venue towards the all-UHV fabrication of vdW heterostructures.

4. Experimental Section

PDMS Stamp Preparation: It used a commercial PDMS elastomer kit (SYLGARD®184), mixing a polymeric base and curing agent at a 10:1 (w/w) ratio in a Petri dish. To prepare the dome-shaped PDMS for stamp 1, the Petri dish was placed upside down for several days, allowing the mixed liquid to slowly form a droplet and cure simultaneously.

Sample Preparation: It exfoliated flakes from bulk crystals onto 285 nm SiO$_2$/Si substrates. Before the exfoliation, the SiO$_2$/Si substrates were ultrasonically cleaned by acetone and 2-propanol, followed by 30 s UV–Ozone treatment.[32] The assembled vdW heterostructures were placed either onto a 285 nm SiO$_2$/Si substrate or alternatively onto pre-evaporated 100 nm/10 nm Au/Ti leads on a 285 nm SiO$_2$/Si substrate and mounted to a standard STM sample plate for the STM measurements. All samples were fabricated in an argon-filled glovebox.

Atomic Force Microscopy: Atomic force microscopy (AFM) experiments were conducted using a Bruker Innova instrument under ambient condition. Contact-mode AFM was used with a setpoint force of ≈6.2 nN and a scan speed of 20 μm s^{-1}. The probing tips used in the experiments were of type Bruker RESPA-20, with a nominal tip radius of 8 nm and a spring constant of 0.9 N m^{-1}.

Scanning Tunneling Microscopy: Scanning tunneling data were acquired at the Centre of Low Temperature Physics in Košice in ultra-high vacuum at a base pressure of ≈1 × 10^{-10} mbar and a base temperature of 1.14 K using a mechanically cut Au tip.

Supporting Information

Supporting Information is available from the Wiley Online Library or from the author.

Conflict of Interest

The authors declare no conflict of interest.

Author Contributions

J.M.C., F.S.T., M.T., and F.L. conceived the research. J.M.C., K.J., T.W., and F.L. designed the experiments. J.Y. grew WTe$_2$ crystals. K.W. and T.T. grew hBN crystals. J.M.C., K.J., and T.W. fabricated the samples. T.S., O.O., and P.S. set up and provided the STM. J.M.C.and T.W. acquired the STM data. J.M.C. and K.J. acquired the optical microscope data and AFM data. J.M.C., K.J., F.S.T., and F.L. wrote the paper. All authors commented on the manuscript. J.M.C., F.S.T., M.T., and F.L. supervised the research.

Data Availability Statement

The data that supports the findings of this study are available in the supplementary material of this article.

Keywords

[1] A. Castellanos-Gomez, X. Duan, Z. Fei, H. R. Gutierrez, Y. Huang, X. Huang, J. Quereda, Q. Qian, E. Sutter, P. Sutter, *Nat. Rev. Methods Primers* **2022**, *2*, 58.

[2] Y. Cao, V. Fatemi, S. Fang, K. Watanabe, T. Taniguchi, E. Kaxiras, P. Jarillo-Herrero, *Nature* **2018**, *556*, 43.

[3] P. Wang, G. Yu, Y. H. Kwan, Y. Jia, S. Lei, S. Klemenz, F. A. Cevallos, R. Singha, T. Devakul, K. Watanabe, T. Taniguchi, S. L. Sondhi, R. J. Cava, L. M. Schoop, S. A. Parameswaran, S. Wu, *Nature* **2022**, *605*, 57.

[4] A. Castellanos-gomez, M. Buscema, R. Molenaar, *2d Mater.* **2014**, *1*, 011002.

[5] F. Pizzocchero, L. Gammelgaard, B. S. Jessen, M. Caridad, L. Wang, J. Hone, P. Bøggild, T. J. Booth, *Nat. Commun.* **2016**, *7*, 11894.

[6] S. Son, Y. J. Shin, K. Zhang, J. Shin, S. Lee, H. Idzuchi, M. J. Coak, H. Kim, J. Kim, J. H. Kim, M. Kim, D. Kim, P. Kim, J.-g. Park, *2D Mater.* **2020**, *7*, 041005.

[7] Y. Wakafuji, R. Moriya, S. Masubuchi, K. Watanabe, T. Taniguchi, T. Machida, *Nano Lett.* **2020**, *20*, 2486.

[8] I. G. Rebollo, F. C. Rodrigues-Machado, W. Wright, G. J. Melin, A. R. Champagne, *2D Mater.* **2021**, *8*, 035028.

[9] J. J. Schwartz, H.-J. Chuang, M. R. Rosenberger, S. V. Sivaram, K. M. McCreary, B. T. Jonker, A. Centrone, *ACS Appl Mater Interfaces* **2019**, *11*, 25578.

[10] Y. Cao, A. Mishchenko, G. L. Yu, E. Khestanova, A. P. Rooney, E. Prestat, A. V. Kretinin, P. Blake, M. B. Shalom, C. Woods, J. Chapman, G. Balakrishnan, I. V. Grigorieva, K. S. Novoselov, B. A. Piot, M. Potemski, K. Watanabe, T. Taniguchi, S. J. Haigh, A. K. Geim, R. V. Gorbachev, *Nano Lett.* **2015**, *15*, 4914.

[11] Z. Qiu, M. Holwill, T. Olsen, P. Lyu, J. Li, H. Fang, H. Yang, M. Kashchenko, K. S. Novoselov, J. Lu, *Nat. Commun.* **2021**, *12*, 70.

[12] Y. Xu, A. Ray, Y.-T. Shao, S. Jiang, K. Lee, D. Weber, J. E. Goldberger, K. Watanabe, T. Taniguchi, D. A. Muller, K. F. Mak, J. Shan, *Nat. Nanotechnol.* **2022**, *17*, 143.

[13] A. M. Goossens, V. E. Calado, A. Barreiro, K. Watanabe, T. Taniguchi, L. M. Vandersypen, *Appl. Phys. Lett.* **2012**, *100*, 073110.

[14] M. R. Rosenberger, H.-J. Chuang, K. M. McCreary, A. T. Hanbicki, S. V. Sivaram, B. T. Jonker, *ACS Appl Mater Interfaces* **2018**, *10*, 10379.

[15] J. Martinez-Castro, D. Mauro, A. Pásztor, I. Gutiérrez-Lezama, A. Scarfato, A. F. Morpurgo, C. Renner, *Nano Lett.* **2018**, *18*, 6696.

[16] I. Cucchi, I. Gutierrez-Lezama, E. Cappelli, S. M. Walker, F. Y. Bruno, G. Tenasini, L. Wang, N. Ubrig, C. Barreteau, E. Giannini, M. Gibertini, A. Tamai, A. F. Morpurgo, F. Baumberger, *Nano Lett.* **2019**, *19*, 554.

[17] K. Kim, M. Yankowitz, B. Fallahazad, S. Kang, H. C. P. Movva, S. Huang, S. Larentis, C. M. Corbet, T. Taniguchi, K. Watanabe, S. K. Banerjee, B. J. LeRoy, E. Tutuc, *Nano Lett.* **2016**, *16*, 1989.

[18] F. Lüpke, D. Waters, S. C. de la Barrera, M. Widom, D. G. Mandrus, J. Yan, R. M. Feenstra, B. M. Hunt, *Nat. Phys.* **2020**, *16*, 526.

[19] F. Lüpke, D. Waters, A. D. Pham, J. Yan, D. G. Mandrus, P. Ganesh, B. M. Hunt, *Nano Lett.* **2022**, *22*, 5674.

[20] D. Shcherbakov, P. Stepanov, D. Weber, Y. Wang, J. Hu, Y. Zhu, K. Watanabe, T. Taniguchi, Z. Mao, W. Windl, J. Goldberger, M. Bockrath, C. N. Lau, *Nano Lett.* **2018**, *18*, 4214.

[21] E. Icking, L. Banszerus, F. Wörtche, F. Volmer, P. Schmidt, C. Steiner, S. Engels, J. Hesselmann, M. Goldsche, K. Watanabe, T. Taniguchi, C. Volk, B. Beschoten, C. Stampfer, *Adv. Electron. Mater.* **2022**, *8*, 2200510.

[22] F. Sigger, H. Lambers, K. Nisi, J. Klein, N. Saigal, A. W. Holleitner, U. Wurstbauer, *Appl. Phys. Lett.* **2022**, *121*, 071102.

[23] B. Parashar, L. Rathmann, H.-J. Kim, I. Cojocariu, A. Bostwick, C. Jozwiak, E. Rotenberg, J. Avila, P. Dudin, V. Feyer, C. Stampfer, B. Beschoten, G. Bihlmayer, C. M. Schneider, L. Plucinski, *Phys. Rev. Mater.* **2023**, *7*, 044004.

[24] B. Fülöp, A. Márffy, S. Zihlmann, M. Gmitra, E. Tóvári, B. Szentpéteri, M. Kedves, K. Watanabe, T. Taniguchi, J. Fabian, C. Schönenberger, P. Makk, S. Csonka, *npj 2D Mater. Appl.* **2021**, *5*, 82.

[25] M. Sui, G. Chen, L. Ma, W. Y. Shan, D. Tian, K. Watanabe, T. Taniguchi, X. Jin, W. Yao, D. Xiao, Y. Zhang, *Nat. Phys.* **2015**, *11*, 1027.

[26] Z. Wang, D. K. Ki, J. Y. Khoo, D. Mauro, H. Berger, L. S. Levitov, A. F. Morpurgo, *Phys. Rev. X* **2016**, *6*, 041020.

[27] N. P. Wilson, K. Lee, J. Cenker, K. Xie, A. H. Dismukes, E. J. Telford, J. Fonseca, S. Sivakumar, C. Dean, T. Cao, X. Roy, X. Xu, X. Zhu, *Nat. Mater.* **2021**, *20*, 1657.

[28] J. Kim, C. Jin, B. Chen, H. Cai, T. Zhao, P. Lee, S. Kahn, K. Watanabe, T. Taniguchi, S. Tongay, M. F. Crommie, F. Wang, *Sci. Adv.* **2017**, *3*, 1700518.

[29] J. Martinez-Castro, T. Wichmann, K. Jin, T. Samuely, Z. Lyu, O. Onufriienko, P. Szabo, F. S. Tautz, M. Ternes, F. Lüpke, *arXiv* **2023**, arXiv:2304.08142 [cond-mat.mes-hall].

[30] M. Onodera, Y. Wakafuji, T. Hashimoto, S. Masubuchi, R. Moriya, Y. Zhang, K. Watanabe, T. Taniguchi, T. Machida, *Sci. Rep.* **2022**, *12*, 21963.

[31] B. Giambattista, A. Johnson, R. V. Coleman, B. Drake, P. K. Hansma, *Phys. Rev. B* **1988**, *37*, 2741.

[32] Y. Huang, E. Sutter, N. N. Shi, J. Zheng, T. Yang, D. Englund, H.-J. Gao, P. Sutter, *ACS Nano* **2015**, *9*, 10612.